Coherent π^0 and η photoproduction on the deuteron

S. S. Kamalov* and L. Tiator
Institut für Kernphysik, Universität Mainz, 55099 Mainz, Germany

C. Bennhold
Center for Nuclear Studies, Department of Physics, The George Washington University, Washington, D.C. 20052

(Received 2 October 1995)

Coherent pion photoproduction, $d(\gamma,\pi^0)d$, is calculated in a coupled channels approach in momentum space using an elementary production operator that includes Born terms, vector meson exchange, and $M1/E2$ Δ-resonance excitation. The final state interaction is treated in the Kerman-McManus-Thaler multiple scattering approach that describes πd elastic scattering well. Differential cross sections are found to agree well with existing (γ,π^0) data. The polarization observables Σ, iT_{11} and the tensor analyzing powers are predicted for forthcoming experiments. A number of transparent relationships between polarization observables and the elementary production operator is derived. Finally, calculations are performed for coherent η photoproduction, $d(\gamma,\eta)d$, in the threshold region which agree well with a very recent Mainz experiment. [S0556-2813(97)04101-0]

PACS number(s): 25.20.Lj, 13.60.Le, 21.45.+v, 25.10.+s

I. INTRODUCTION

For a long time, coherent pion photoproduction on the deuteron has been studied as a source of information on π^0 photoproduction off the neutron. In the beginning, the impulse approximation was the main instrument for this undertaking. However, in contrast to charged pion photoproduction where the largest contribution comes from the well-known Kroll-Ruderman amplitude, the isoscalar π^0 amplitude on the deuteron target is drastically reduced due to an accidental cancelation between leading terms. Therefore, the contributions from pion rescattering or final state interaction (FSI) become extremely important. This dramatic effect from pion rescattering with charge exchange contributions was first found by Koch and Woloshyn [1] and then verified by Bosted and Laget [2] in studies of coherent pion photoproduction on the deuteron in the threshold region.

With increasing photon energy the contribution from the direct term (without rescattering) becomes very large due to the dominance of the Δ-resonance contribution and finally dominates the cross section. In the Δ-resonance region the main mechanism of FSI is elastic pion scattering; the contributions from the charge exchange reactions become small. In recent years, the three-body approach has been employed for the description of FSI. By solving the Faddeev equations it is possible to take into account the coupling with the breakup and pion absorption channels. In this framework considerable progress has been achieved in the description of pion-deuteron elastic scattering (see, for example, the review of Ref. [3]). Very recently, Wilhelm and Arenhövel [4,5] used an approach of $NN-N\Delta$ coupled channels for describing deuteron photodisintegration, $\gamma d \to pn$ and coherent pion photoproduction,

$$\gamma + d \to \pi^0 + d. \tag{1}$$

In another approach, recently developed for reaction (1) by Garcilazo and de Guerra [6], relativistic Feynman diagrams have been evaluated. Using the spectator-on-mass-shell prescription, differential cross sections and polarization observables have been calculated in the energy region from threshold up to 1 GeV. Blaazer [7], on the other hand, used a Faddeev approach to the πNN system to describe pion rescattering in the final state.

This paper is the continuation of our previous work which was devoted to pion scattering [8,9] and pion photoproduction [10,11] on very light nuclei. Using a microscopic approach based on the KMT multiple scattering approach [12] in momentum space we have achieved a good description of pion scattering on deuteron and ^{3}He and pion photoproduction on ^{3}He.

In paper I [8], we demonstrated that a microscopic description of elastic πd scattering in the framework of the multiple scattering theory is able to describe the differential cross section and polarization observables equally well as in the Faddeev approach. Furthermore, our multiple scattering approach proved to be very transparent, simplifying a comparison of the pion interaction with heavier nuclei. We believe the same rational holds in the case of coherent π^0 photoproduction.

Very recently, interest in the physics with eta mesons has grown significantly. This relatively new field of theoretical and experimental studies is promising to be very useful to obtain a more global picture of the meson-nuclear interaction. On the other hand, these studies could give important information on the excitation of nucleon resonances in nuclei [like the $S_{11}(1535)$ and the $D_{13}(1525)$]. Eta photoproduction on the deuteron is of special interest since, due to isospin selection rules a measurement of this process should allow us to completely determine the proton and neutron electromagnetic amplitudes and to separate the isospin components of the nucleon resonances.

*Permanent address: Laboratory of Theoretical Physics, JINR Dubna, Head Post Office Box 79, SU-101000 Moscow, Russia.

 © 1997 The American Physical Society

Unfortunately, despite its long history, the experimental data available for the meson photoproduction processes on the deuteron are not of as high a quality as the ones for, i.e., elastic pion scattering. However, with the new accelerators at Mainz, Bonn, Saskatoon and, in the near future, CEBAF we hope that such data will be available soon.

The basic ingredients of our formalism based on the multiple scattering approach and coupled-channels method are given in Sec. II. In Sec. III we present the main expressions for the differential cross section and polarization observables. Our results for coherent π^0 photoproduction are discussed in Sec. IV. In Sec. V, we will complete our analysis with the investigation of coherent eta photoproduction on the deuteron. A summary and conclusions are given in Sec. VI.

II. BASIC INGREDIENTS OF THE THEORY

To obtain the amplitude of pion photoproduction on nuclei one may start, as in pion scattering, with the amplitude of the elementary process and the use of multiple scattering theory [12,13]. An extension of the KMT approach [12] to the case of nuclear pion photoproduction leads to the following expression for the T matrix:

$$T_\gamma(E)=\sum_{j=1}^{A}\tau_j^\gamma+\sum_{i\neq j}^{A}\sum_{j=1}^{A}\tau_i G_0(E)\tau_j^\gamma + \sum_{k\neq i}^{A}\sum_{j\neq i}^{A}\sum_{j=1}^{A}\tau_k G_0(E)\tau_i G_0(E)\tau_j^\gamma+\cdots, \quad (2)$$

where τ_i and τ_j^γ describe the pion scattering and pion photoproduction on bound nucleons, respectively, and $G_0(E)$ is the Green's function for a free pion-nuclear system. Together with the equations for the pion-nuclear scattering T matrix (see paper I), Eq. (2) can be rewritten as a system of integral equations:

$$T_\gamma(E)=U_\gamma(E)+T'(E)G_0(E)U_\gamma(E), \quad (3a)$$

$$T'(E)=U'(E)+U'(E)G_0(E)T'(E), \quad (3b)$$

where

$$T'(E)=\frac{A-1}{A}T(E),\quad U'(E)=\frac{A-1}{A}\sum_{j=1}^{A}\tau_j(E),$$

$$\text{and}\quad U_\gamma(E)=\sum_{j=1}^{A}\tau_j^\gamma(E). \quad (4)$$

For a consistent derivation of the pion photoproduction amplitude from Eq. (3) we will use the same approximations as in pion scattering. First in the spectral decomposition of the Green's function only the deuteron ground state is retained, *neglecting the contributions from the coupling with the break-up channels*. As we have seen in paper I, this approximation is a reasonable starting point to study pion-nuclear scattering. However, as we will see below, near threshold for isoscalar nuclei like the deuteron the ground state contribution is very small and the coupling to the breakup channels becomes important. Second we use the free elementary t matrix, $\tau^\gamma(E)\approx t^\gamma(\omega)$. The last assumption is called *modified impulse approximation* where the connection between pion-nucleon (ω) and pion-nuclear (E) energies is the same as in elastic pion scattering (three-body choice):

$$\omega=E+m_\pi+M_N-\left[(m_\pi+M_N)^2+\frac{(\vec{q}+\vec{k})^2}{16}\right]^{1/2} -\left[M_N^2+\frac{(\vec{q}+\vec{k})^2}{16}\right]^{1/2}, \quad (5)$$

where m_π and M_N are the pion and nucleon masses, $\vec{k}$ and $\vec{q}$ are the photon and pion momenta, respectively. As we have shown in paper I, this choice improves the impulse approximation in pion scattering.

Finally, using these two approximations for the nuclear pion photoproduction amplitude we get an expression in the *distorted wave impulse approximation* (DWIA). In momentum space it can be presented as

$$F^{(\lambda)}_{M_f M_i}(\vec{q},\vec{k})=V^{(\lambda)}_{M_f M_i}(\vec{q},\vec{k})-\frac{1}{(2\pi)^2}\times\sum_{M_f'}\int\frac{d\vec{q}'}{\mathcal{M}(q')}\frac{F'_{M_f M_f'}(\vec{q},\vec{q}')V^{(\lambda)}_{M_f' M_i}(\vec{q}',\vec{k})}{E(q)-E(q')+i\epsilon}, \quad (6)$$

where the amplitudes $F^{(\lambda)}_{M_f M_i}$ and $F'_{M_f M_f'}$ are connected with the $T_\gamma(E)$ and $T'(E)$ matrixes in Eq. (3) via relations

$$F^{(\lambda)}_{M_f M_i}(\vec{q},\vec{k})=-\frac{\sqrt{\mathcal{M}(q)\mathcal{M}(k)}}{2\pi}\langle\pi(\vec{q}),f|T_\gamma(E)|i,\gamma(\vec{k}\lambda)\rangle, \quad (7a)$$

$$F'_{M_f M_f'}(\vec{q},\vec{q}')=-\frac{\sqrt{\mathcal{M}(q)\mathcal{M}(q')}}{2\pi}\times\langle\pi(\vec{q}),f|T'(E)|f',\pi(\vec{q}')\rangle. \quad (7b)$$

In Eqs. (6)–(7b) $\lambda=\pm1$ is the photon polarization, $|i\rangle,|f\rangle$, and $|f'\rangle$ are the deuteron ground state which differs only by projection of the deuteron's spin, M_i, M_f and M_f'. The relativistic pion-nuclear and photon-nuclear reduced masses are given by $\mathcal{M}(q)=E_\pi(q)E_A(q)/E(q)$ and $\mathcal{M}(k)=kE_A(k)/E(k)$, where $E=E(q)=E(k)$ is the pion-nuclear (or photon-nuclear) total energy in the pion-nuclear (πA) c.m. system.

Note that the main difference compared to the standard DWIA approach (which is not appropriate for the deuteron) is the factor $(A-1)/A$ in the T' matrix. This factor avoids double counting of pion rescattering on one and the same nucleon. Such effects are already included in the elementary amplitude. Another difference is that Eq. (6) includes not only coherent (non-spin-flip) pion rescattering but also incoherent spin-flip transitions which change the projection of the spin of the deuteron.

In the framework of the *plane wave impulse approximation* (PWIA) the pion photoproduction amplitude is equal to the first term of Eq. (6) which is expressed in terms of the elementary pion-nucleon photoproduction $t^\gamma(\omega)$ matrix or amplitude $f^{(\lambda)}$:

$$V^{(\lambda)}_{M_f M_i}(\vec{q},\vec{k}) = -\frac{\sqrt{\mathcal{M}(q)\mathcal{M}(k)}}{2\pi} \times \left\langle \pi(\vec{q}), f \left| \sum_{j=1}^{A} t_j^{\gamma}(\omega) \right| i, \gamma(\vec{k}\lambda) \right\rangle, \quad (8a)$$

$$\langle \vec{q},\vec{p}\,' | t^{\gamma}(\omega) | \vec{p},\vec{k}\lambda \rangle = -\frac{2\pi}{\sqrt{\mu(q,p')\mu(k,p)}} f^{(\lambda)}(\omega,\theta^*_\pi) \times \delta(\vec{p}\,' + \vec{q} - \vec{p} - \vec{k}), \quad (8b)$$

where relativistic pion-nuclear and photon-nuclear reduced masses are $\mu(q,p') = E_\pi(q)E_N(p')/\omega$ and $\mu(k,p) = kE_N(p)/\omega$, $\vec{p}$ and $\vec{p}\,'$ are the nucleon momenta in the initial and final states (in πA c.m. system), respectively.

The relativistically invariant amplitude $f^{(\lambda)}$, in the pion-nucleon (πN) c.m. system has the standard CGLN form [14]

$$f^{(\lambda)}(\omega,\theta^*_\pi) = iF_1 \vec{\sigma}\cdot\vec{\epsilon}_\lambda + F_2 \vec{\sigma}\cdot\hat{\vec{q}}\,\vec{\sigma}\cdot[\hat{\vec{k}}\times\vec{\epsilon}_\lambda] + iF_3 \vec{\sigma}\cdot\hat{\vec{k}}\,\hat{\vec{q}}\cdot\vec{\epsilon}_\lambda + iF_4 \vec{\sigma}\cdot\hat{\vec{q}}\,\hat{\vec{q}}\cdot\vec{\epsilon}_\lambda, \quad (9)$$

where $\hat{\vec{q}}$ and $\hat{\vec{k}}$ are the unit vectors for the pion and photon momenta in the πN c.m. system, θ^*_π is the pion angle in the same system. All these variables can be expressed in an arbitrary frame via the standard Lorentz transformation (see Ref. [11]).

In nuclear applications, it is convenient to divide the amplitude in Eq. (9) into non-spin-flip (f_2) and spin-flip (f_1, f_3, f_4) amplitudes

$$f^{(\lambda)} = if_1 \vec{\sigma}\cdot\vec{\epsilon}_\lambda + f_2[\hat{\vec{q}}\times\hat{\vec{k}}]\cdot\epsilon_\lambda + if_3 \vec{\sigma}\cdot\hat{\vec{k}}\,\hat{\vec{q}}\cdot\vec{\epsilon}_\lambda + if_4 \vec{\sigma}\cdot\hat{\vec{q}}\,\hat{\vec{q}}\cdot\vec{\epsilon}_\lambda. \quad (10)$$

These are connected to the standard CGLN amplitudes via

$$f_1 = F_1 - F_2\cos\theta^*_\pi, \quad f_2 = F_2, \quad f_3 = F_3 + F_2, \quad f_4 = F_4. \quad (11)$$

In terms of the lowest s- and p-wave multipoles, the amplitudes f_i can be expressed as

$$f_1 = E_{0+} + \cos\theta^*_\pi(3E_{1+} + M_{1+} - M_{1-}), \quad (12a)$$

$$f_2 = 2M_{1+} + M_{1-}, \quad (12b)$$

$$f_3 = 3E_{1+} - M_{1+} + M_{1-}, \quad (12c)$$

$$f_4 = 0. \quad (12d)$$

In our calculation, we use the unitary version of the Blomqvist-Laget amplitude [15,16] for the elementary amplitude which contains contributions from Born and ω-exchange terms. The dominant Δ-resonance contribution is described by the real and imaginary parts of the resonant $M^{\Delta}_{1+}(\omega)$ and $E^{\Delta}_{1+}(\omega)$ multipoles that are added to the background terms in a unitarized way. Here we want to remind that in accordance with the Blomqvist-Laget approach the pion photoproduction operator used for nuclear applications is obtained after a nonrelativistic reduction to order $(\vec{p}/M_N)^2$ of the relativistic and gauge invariant amplitude. Due to the reduction procedure gauge invariance is no longer exactly fulfilled but to order $(\vec{p}/M_N)^2$, consistent with the nonrelativistic reduction. It was shown in Refs. [15,16] that up to photon laboratory energies of about 500 MeV this approximation is well suitable and agrees well with the experimental data for the elementary reaction.

Embedding a gauge invariant one-body operator in a nucleus in the framework of the impulse approximation, however, will always violate gauge invariance due to binding or off-shell effects. This is well known in electron scattering where *meson exchange currents* (MEC) have to be included. As it was shown in our previous work [17] one way to construct a gauge invariant nuclear pion photoproduction amplitude is using minimal substitution of the electromagnetic field in the nuclear pion emission amplitude and in the nuclear wave function, satisfying the Schrödinger equation with the nuclear Hamiltonian $H_A = T + V_A$.

Minimal substitution in the kinetic term T gives the standard nucleon pole terms of the elementary (one-body) pion photoproduction amplitude. In addition, a two-body operator appears, describing the process where the photon is absorbed on one nucleon and the pion is emitted from another nucleon. Such a two-body mechanism is not included in Eq. (2). As it was shown in Ref. [17] in the case ^{3}He$(\gamma,\pi^+)^3$H this two-body mechanism can be important at high energies and backward angles. On the other hand, in the case of the deuteron the corresponding contribution from minimal substitution in the nuclear wave functions in the initial and final states cancel each other almost exactly. A similar cancelation has been found in Ref. [18] in pion-deuteron elastic scattering.

Further two-body contributions could appear due to minimal substitution in the nuclear potential V_A which has essentially a one boson exchange nature. In this way we can generate the meson exchange currents of pion photoproduction. This issue has not been studied in detail for pion photoproduction and is beyond the realm of our paper. A detailed discussion of this problem can be found in Ref. [19], where such MEC contributions are found to be of higher order in p/M_N. In the following our considerations will be based on the conventional approach without MEC degrees of freedom.

Finally, we mention the so-called *factorization approximation* in the treatment of nucleon Fermi motion. We have developed the formalism for the exact treatment of the nucleon momentum dependence in the elementary amplitude using a multidimensional integration in Eqs. (7a) and (7b). However, similar to our previous studies [20,21] the substitution

$$\vec{p} \to \vec{p}_{\rm eff} = -\frac{\vec{k}}{A} - \frac{A-1}{2A}(\vec{k} - \vec{q}) = -\frac{\vec{k}}{2} - \frac{1}{4}\vec{Q} \quad (13)$$

works very well quantitatively and provides an excellent approximation. This result is based on the fact that in case of a Gauss wave function, which roughly reproduces the dominant S-wave part of the deuteron ground state, the replacement (13) gives an exact treatment for the linear $\vec{p}/2M$ terms in the elementary amplitude.

III. POLARIZATION OBSERVABLES

Polarization observables have the promise of opening a new field in the electromagnetic production of pions from protons and nuclear targets. Since many of these observables contain interference terms, small but important amplitudes can be investigated in a unique way.

To define our polarization observables we choose the system of coordinates corresponding to the *Madison Convention* [22]: a right-handed coordinate system where the positive z axis is along the photon beam direction and the y axis is along the vector $[\vec{k}\times\vec{q}]$.

In this paper, we focus only on single polarization observables that appear in π^0 photoproduction with a polarized beam and an unpolarized target, or an unpolarized beam and a polarized target. In both cases five polarization observables can be measured.

The photon asymmetry

$$\Sigma=\frac{d\sigma/d\Omega^{\perp}-d\sigma/d\Omega^{(\parallel)}}{d\sigma/d\Omega^{\perp}+d\sigma/d\Omega^{(\parallel)}}, \tag{14}$$

where $\perp$ ($\parallel$) refers to a photon linearly polarized perpendicular (parallel) to the reaction plane and four *analyzing powers* (the vector, iT_{11}, and three tensor ones, T_{20},T_{21},T_{22})

$$T_{k\kappa}=\frac{\mathrm{Tr}(F\tau_{k\kappa}F^{\dagger})}{\mathrm{Tr}(FF^{\dagger})}. \tag{15}$$

In Eq. (15), the spherical tensor operator $\tau_{k\kappa}$ is defined as

$$\langle JM'|\tau_{k\kappa}|JM\rangle=\hat{J}\hat{k}(-1)^{J+M'}\begin{pmatrix} J & J & k \\ M & -M' & \kappa\end{pmatrix} \tag{16}$$

with a Wigner $3j$ symbol and $\hat{J}=\sqrt{2J+1}$.

From the partial wave decomposition of the electromagnetic vector potential [13] it follows that the pion photoproduction matrix elements, $F^{(\lambda)}_{M_fM_i}$, can be divided into magnetic and electric components which are both independent of the photon polarization $\lambda=\pm1$:

$$F^{(\lambda)}_{M_fM_i}=F^{(M)}_{M_fM_i}+\lambda F^{(E)}_{M_fM_i}. \tag{17}$$

Similar to the formalism in pion scattering, one can present the photoproduction matrix in the following form:

$$F^{(\lambda)}_{M_fM_i}=\begin{pmatrix} F^{(\lambda)}_{++} & F^{(\lambda)}_{0+} & F^{(\lambda)}_{-+} \\ F^{(\lambda)}_{+0} & F^{(\lambda)}_{00} & F^{(\lambda)}_{-0} \\ F^{(\lambda)}_{+-} & F^{(\lambda)}_{0-} & F^{(\lambda)}_{--}\end{pmatrix}=\begin{pmatrix} \mathcal{A}_M & \mathcal{B}_M & \mathcal{C}_M \\ \mathcal{D}_M & \mathcal{E}_M & -\mathcal{D}_M \\ \mathcal{C}_M & -\mathcal{B}_M & \mathcal{A}_M\end{pmatrix}$$
$$+\lambda\begin{pmatrix} \mathcal{A}_E & \mathcal{B}_E & \mathcal{C}_E \\ \mathcal{D}_E & 0 & \mathcal{D}_E \\ -\mathcal{C}_E & \mathcal{B}_E & -\mathcal{A}_E\end{pmatrix}, \tag{18}$$

where the signs $+,0,-$ correspond to the deuteron spin projections $M_{i(f)}=+1,0,-1$, respectively. Note that the structure of the magnetic part of matrix (18) is similar to the *Robson* matrix [23] which was discussed in the case of elastic pion scattering [17]. The main difference appears in the electric part, whose contribution is much smaller. Therefore, the behavior of the differential cross section and the single polarization observables is mainly determined by the five magnetic amplitudes. We point out that the $\mathcal{C}_E$ amplitude vanishes in PWIA; it has contributions due only to pion rescattering.

Calculating the expectation values of the operator $\tau_{k\kappa}$ for $k=\kappa=0$, the differential cross section and photon asymmetry can be written as

$$\frac{d\sigma}{d\Omega}=\frac{d\sigma_M}{d\Omega}+\frac{d\sigma_E}{d\Omega}, \tag{19a}$$

$$\frac{d\sigma_M}{d\Omega}=\frac{2q}{3k}(|\mathcal{A}_M|^2+|\mathcal{B}_M|^2+|\mathcal{C}_M|^2+|\mathcal{D}_M|^2+\tfrac{1}{2}|\mathcal{E}_M|^2), \tag{19b}$$

$$\frac{d\sigma_E}{d\Omega}=\frac{2q}{3k}(|\mathcal{A}_E|^2+|\mathcal{B}_E|^2+|\mathcal{C}_E|^2+|\mathcal{D}_E|^2), \tag{19c}$$

$$\Sigma=\frac{d\sigma_M/d\Omega-d\sigma_E/d\Omega}{d\sigma_M/d\Omega+d\sigma_E/d\Omega}. \tag{19d}$$

Similarly, the vector and tensor analyzing powers can be divided into magnetic and electric parts

$$T_{k\kappa}=T^{(M)}_{k\kappa}+T^{(E)}_{k\kappa}. \tag{20}$$

The expression for $T^{(M)}_{k\kappa}$ in terms of the $\mathcal{A}_M,\ldots,\mathcal{E}_M$ amplitudes are the same as in pion scattering:

$$iT^{(M)}_{11}=\sqrt{2/3}\mathrm{Im}[\mathcal{D}^*_M(\mathcal{A}_M-\mathcal{C}_M)-\mathcal{B}^*_M\mathcal{E}_M)]/a(\theta_\pi), \tag{21a}$$

$$T^{(M)}_{20}=\frac{\sqrt{2}}{3}(|\mathcal{A}_M|^2+|\mathcal{B}_M|^2+|\mathcal{C}_M|^2-2|\mathcal{D}_M|^2-|\mathcal{E}_M|^2)/a(\theta_\pi), \tag{21b}$$

$$T^{(M)}_{21}=-\sqrt{2/3}\mathrm{Re}[\mathcal{D}^*_M(\mathcal{A}_M-\mathcal{C}_M)+\mathcal{B}^*_M\mathcal{E}_M)]/a(\theta_\pi), \tag{21c}$$

$$T^{(M)}_{22}=\frac{1}{\sqrt{3}}[2\mathrm{Re}(\mathcal{A}^*_M\mathcal{C}_M)-|\mathcal{B}_M|^2]/a(\theta_\pi), \tag{21d}$$

$$a(\theta_\pi)=\frac{k}{q}\frac{d\sigma}{d\Omega}. \tag{21e}$$

For the electric part of the analyzing powers we obtain

$$iT^{(E)}_{11}=\sqrt{2/3}\mathrm{Im}[\mathcal{D}^*_E(\mathcal{A}_E+\mathcal{C}_E)]/a(\theta_\pi), \tag{22a}$$

$$T^{(E)}_{20}=\frac{\sqrt{2}}{3}(|\mathcal{A}_E|^2+|\mathcal{B}_E|^2+|\mathcal{C}_E|^2-2|\mathcal{D}_E|^2)/a(\theta_\pi), \tag{22b}$$

$$T^{(E)}_{21}=-\sqrt{2/3}\mathrm{Re}[\mathcal{D}^*_E(\mathcal{A}_E+\mathcal{C}_E)]/a(\theta_\pi), \tag{22c}$$

$$T^{(E)}_{22}=-\frac{1}{\sqrt{3}}[2\mathrm{Re}(\mathcal{A}^*_E\mathcal{C}_E)-|\mathcal{B}_E|^2]/a(\theta_\pi). \tag{22d}$$

Finally, we present expressions for the $\mathcal{A},\mathcal{B}$, etc. amplitudes obtained: (1) in the plane wave impulse approximation

and (2) by taking into account only contributions from the S component and its interference with the D component of the deuteron wave function. Then the Robson amplitudes can be expressed solely through the elementary amplitudes $f_1,\ldots,f_4$ from Eq. (10) and the radial integrals $R_{l'l}$ (introduced in paper I):

$$R^{(L)}_{l'l}(Q)=\int rU_{l'}(r)j_L\left(\frac{Qr}{2}\right)U_l(r), \tag{23}$$

where U_l is the deuteron radial wave function $j_L(z)$ is the spherical Bessel function, and $\{l,l'\}=0,2$. This yields

$$\mathcal{A}_M\cong\sqrt{2}f_2\sin\theta^*_\pi\left[R^{(0)}_{00}-\frac{1}{2\sqrt{2}}(1+3\cos2\Theta)R^{(2)}_{02}\right]W_A, \tag{24a}$$

$$\mathcal{B}_M\cong\left(f_1R_S+\frac{3}{\sqrt{2}}f_2\sin\theta^*_\pi\sin2\Theta R^{(2)}_{02}\right)W_A, \tag{24b}$$

$$\mathcal{C}_M\cong-\frac{3}{2}f_2\sin\theta^*_\pi(1-\cos2\Theta)R^{(2)}_{02}W_A, \tag{24c}$$

$$\mathcal{D}_M\cong-\left(f_1R_S-\frac{3}{\sqrt{2}}f_2\sin\theta^*_\pi\sin2\Theta R^{(2)}_{02}\right)W_A, \tag{24d}$$

$$\mathcal{E}_M\cong\sqrt{2}f_2\sin\theta^*_\pi\left[R^{(0)}_{00}+\frac{1}{\sqrt{2}}(1+3\cos2\Theta)R^{(2)}_{02}\right]W_A, \tag{24e}$$

$$\mathcal{A}_E\cong-\sqrt{2}\sin\theta^*_\pi\left[(f_3+f_4\cos\theta^*_\pi)R_S+\frac{3}{\sqrt{2}}f_Q\cos\Theta R^{(2)}_{02}\right]W_A, \tag{24f}$$

$$\mathcal{B}_E=\mathcal{D}_E\cong-\left[(f_1+f_4\sin^2\theta^*_\pi)R_S-\frac{3}{\sqrt{2}}f_Q\sin\theta^*_\pi\sin\Theta R^{(2)}_{02}\right]W_A, \tag{24g}$$

where we have used the following notations:

$$R_S(Q)=R^{(0)}_{00}(Q)+\frac{1}{\sqrt{2}}R^{(2)}_{02}(Q), \tag{25a}$$

$$f_Q=\frac{q}{Q}(f_1+f_3\cos\theta^*_\pi+f_4)-\frac{k}{Q}(f_3+f_4\cos\theta^*_\pi), \tag{25b}$$

$$\cos\Theta=\frac{1}{Q}(k-q\cos\theta_\pi). \tag{25c}$$

In Eqs. (24a)–(25c) θ^*_π is the pion angle in πN c.m. system, $\vec{Q}=\vec{k}-\vec{q}$ is the nuclear momentum transfer. The kinematical factor W_A can easily be obtained from Eq. (8).

As we will see below, the expressions (24a)–(24g) are very useful for a qualitative as well as a quantitative understanding of the polarization observables. The complete expressions (including complete contributions from the deuteron D-state component) are given in the Appendix.

IV. RESULTS AND DISCUSSION

A. Differential cross section

We begin our discussion with the results for the differential cross section. Using our formalism described above we will show that it reproduces the well-known results for the coherent π^0 photoproduction at threshold and in the Δ-resonance region.

In general, pion photoproduction near threshold is dominated by the spin-flip amplitude with the leading multipole E_{0+}. However, neutral pion photoproduction is comparable to the situation with the scattering length in elastic pion-deuteron scattering (see paper I): the isoscalar part of the s-wave multipole is one order of magnitude smaller than the isovector one. Therefore, the PWIA approach is not valid at threshold and contributions from pion rescattering with charge exchange become very important [1,2]. For this two-step process the corresponding contribution to the total amplitude can be estimated by using the first iteration of Eq. (3)

$$F^{(\lambda)}_{\text{Resc.}}=\frac{\mathcal{M}_{\pi d}}{\mu_{\pi N}}W_A\left\langle d\left|e^{i\vec{r}\cdot(\vec{k}+\vec{q})/2}\frac{e^{iq_0r}}{r}\sum_{i\neq j}f_{\pi N}(i)f^{(\lambda)}(j)\right|d\right\rangle, \tag{26}$$

where $\mathcal{M}_{\pi d}$ and $\mu_{\pi N}$ are the reduced masses for the πd and πN systems, respectively, $|d\rangle$ is the deuteron ground state, and q_0 is the on shell momentum of the pion in the intermediate state.

In the limit of $q\to0$, the elementary amplitudes for πN scattering, $f_{\pi N}$, and pion photoproduction, $f^{(\lambda)}$, become constant and the total amplitude (with direct and rescattering contributions) can be reduced to the expression [24]

$$F^{(\lambda)}\approx W_AR^{(0)}_{00}(Q)\left[(E^{\pi^0p}_{0+}+E^{\pi^0n}_{0+})+\frac{\mathcal{M}_{\pi d}}{\mu_{\pi N}}\left\langle\frac{1}{r}\right\rangle a^{\pi^0\pi^+}_{\pi N}(E^{\pi^+n}_{0+}-E^{\pi^-p}_{0+})\right] \tag{27}$$

with the pion-nucleon scattering length $a^{\pi^0\pi^+}_{\pi N}=-a^{\pi^0\pi^-}_{\pi N}=\sqrt{2}(a_1-a_3)/3=0.122/m_\pi$ and $\langle1/r\rangle=0.65/m_\pi$. In Eq. (27), the $E^{\pi^0N}_{0+}$ multipoles for π^0 photoproduction are much smaller than the Kroll-Ruderman multipole $E^{\pi^\pm N}_{0+}$ thus the rescattering terms are comparatively enhanced.

In Fig. 1 we show our calculations for the total and differential cross section in the threshold region. In this region the contribution of elastic rescattering (without charge exchange) is very small. This is due to the small size of the isoscalar part of the πN scattering amplitude. On the other hand, due to its large isovector part and also due to the large $E^{\pi^\pm N}_{0+}$ multipole, the role of the charge exchange process becomes very important. In the upper figure the reduced cross section is compared with a recent reanalysis [25] of an earlier Saclay measurement. The full calculations are about 15% larger than the experimental data. The same results have recently been obtained by Garcilazo and Guerra [6] using a

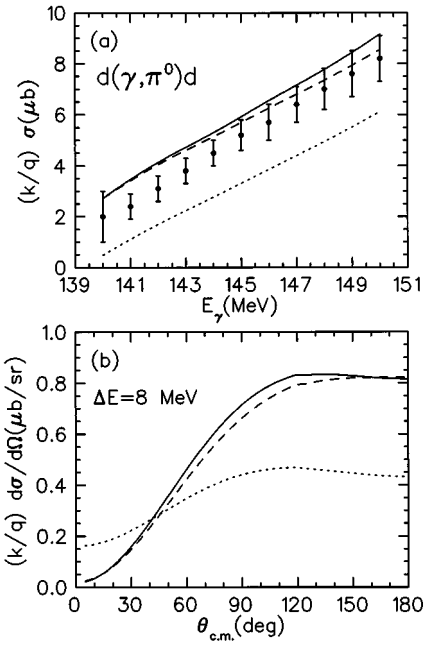

FIG. 1. (a) Reduced total cross section as a function of the photon lab energy near threshold. The dotted curves are the PWIA results, the dashed and solid curves are the calculations including pion charge exchange without and with elastic pion rescattering, respectively. The data are from Ref. [25]. (b) Reduced differential cross section for the photon excess energy in the lab frame above threshold, $\Delta E = E_\gamma - E_\gamma^{\rm thr} = 8$ MeV. The notation of the curves is the same as in (a).

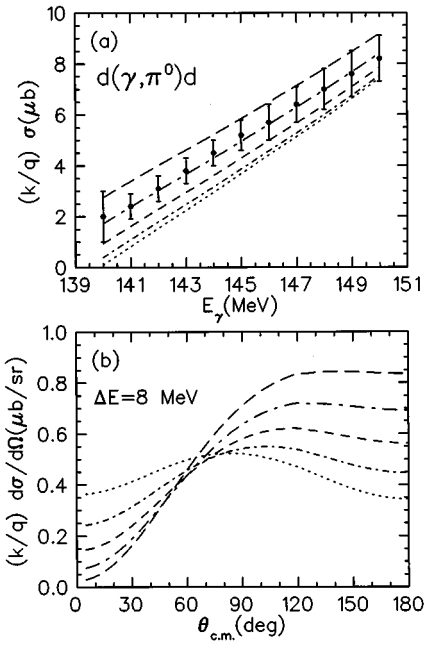

FIG. 2. (a) Sensitivity of the reduced total cross section on the isospin (+) amplitude in the direct term. From top to bottom the $E_{0+}^{(+)}$ s-wave amplitude has been taken as $-1, -0.5, 0, +0.5, +1$ in units of $10^{-3}/m_\pi$. All curves have been calculated with full rescattering including the SCE contribution. The data are from Ref. [25]. (b) Reduced differential cross section for the photon excess energy in the lab frame above threshold, $\Delta E = E_\gamma - E_\gamma^{\rm thr} = 8$ MeV. The notation of the curves is the same as in (a).

Feynman diagram method with a pure pseudovector πNN coupling. Calculations by Bosted and Laget [2] are about 15% lower than ours and agree better with the experiment.

The authors of Ref. [6] argue that the main reason of their disagreement with the experiment could be due to the contributions from third- and higher-order scattering terms. However, our calculations (compare dashed and solid curves in Fig. 1) show that such contributions usually increase the cross section because of the attractive nature of the pion-nuclear interaction in the threshold region.

In the lower part of Fig. 1 we show calculations for the differential cross section at $\Delta E = E_\gamma - E_\gamma^{\rm thr} = 8$ MeV. Here we see that the interference between direct and rescattering terms is strongly angle dependent, leading to an increase in the differential cross section by about a factor of two at backward angles.

Recent developments in π^0 photoproduction on the proton [26,27] that indicate large deviations from the old low energy theorem (LET) predictions suggest that such effects could also be visible in coherent photoproduction on the deuteron. In the direct term only the isospin (+) amplitude appears which is proportional to the sum of the proton and neutron amplitudes, $E_{0+}^{(+)} = [E_{0+}(\pi^0 p) + E_{0+}(\pi^0 n)]/2$. While PV Born terms predict this amplitude to be constant in the threshold region with a value close to the old LET, $E_{0+}^{(+)} = -1.0 \times 10^{-3}/m_\pi$, the new experiments on the proton show an energy dependent function with a cusp effect at the charged pion threshold. Using isospin symmetry, with this new experimental data and the older values for $(\gamma, \pi^\pm)$ [28] we find values for $E_{0+}^{(+)}$ from -1.5 to $+1.5$ in units of $10^{-3}/m_\pi$. Predictions from chiral perturbation theory give positive values for this amplitude that vary between the neutral and charged thresholds in the range of $(0.5-1.2) \times 10^{-3}/m_\pi$ [29]. In Fig. 2, we show the influence of this isospin (+) amplitude on the total and differential cross section of coherent pion photoproduction on the deuteron. Even though the direct term is not dominant in this reaction, a significant sensitivity can be seen because of the interference with the pion rescattering channel. Comparing our calculations with the total cross section data in Fig. 2(a) leads to a preferred value of $-0.5 \times 10^{-3}/m_\pi$. As demonstrated in Fig. 2(b), a determination of $E_{0+}^{(+)}$ should be much easier using angular distributions, where one can easily distinguish different values in the forward-backward angular asymmetry.

With increasing photon energy the contributions from p-wave multipoles become stronger, due mostly to the excitation of the Δ resonance. Figure 3 illustrates the role of the individual parts of the elementary photoproduction amplitude: the Born+ω-exchange terms (dotted curves), the Δ-resonance contribution (dashed curves), and the total amplitude (solid curves). The Born and ω-exchange diagrams are essential at forward and backward angles. In this region only the f_1 amplitude remains which contains the nonresonant E_{0+} and M_{1-} multipoles as well as the resonant M_{1+}^Δ and E_{1+}^Δ amplitudes. Around $\theta_\pi = 90°$, the Δ-resonance contribution dominates due to the magnitude of the coherent contribution from the non-spin-flip amplitude f_2.

In comparison to the available data the overall agreement is satisfactory. An exception may be the large disagreement

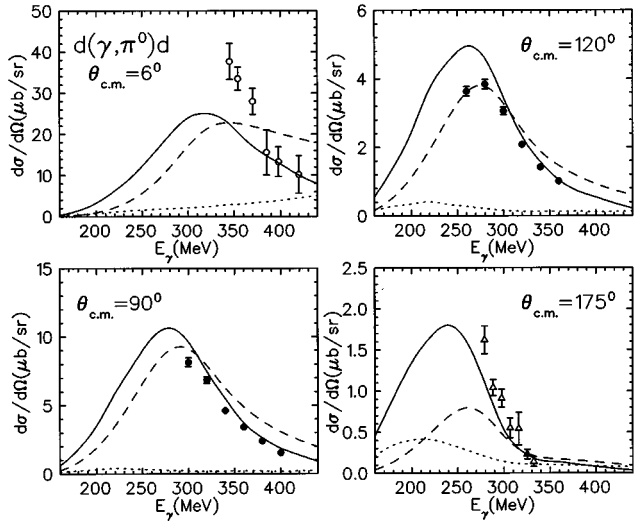

FIG. 3. Energy dependence of the differential cross section at fixed angles $\theta_\pi = 6°$, 90°, 120°, and 175°. The dotted and dashed curves are the calculations only with Born+ω-exchange and Δ contributions, respectively. Solid curves are the results of the full calculations. Experimental data are from Refs. [30] (o), [31] (●), and [32] (△).

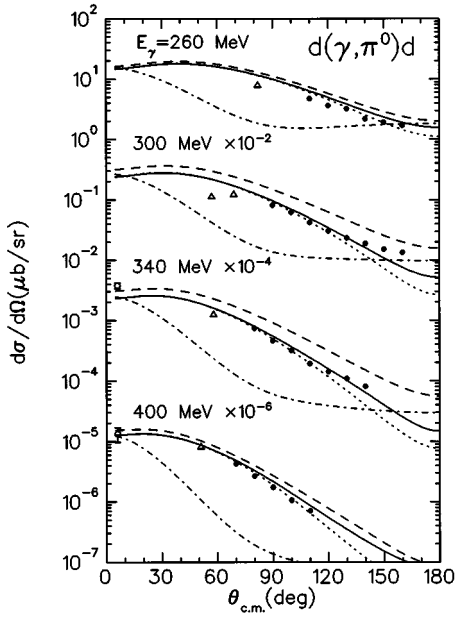

FIG. 4. Angular distribution at fixed photon lab energy $E_\gamma =$ 260, 300, 340, and 400 MeV. The dashed and solid curves are PWIA and full calculations. The dash-dotted and dotted curves are the calculations without non-spin-flip and without deuteron D-state, respectively. Experimental data are from Refs. [30] (o), Refs. [31] (●), and [33] (△).

in the forward direction with the data from Ref. [33] with rather large error bars. The best description of the experimental measurements is achieved at $\theta_\pi = 90°$, where the Δ contribution dominates. Together with our earlier results obtained for ^{3}He and p-shell nuclei, this gives us confidence in the treatment of Δ propagation in nuclei. In order to draw further conclusions more precise experiments are needed, in particular at extreme angles where the Δ contribution is weaker.

Figure 4 shows the differential cross sections at $E_\gamma = 260$–400 MeV. Here we illustrate the role of the spin-flip contribution (dash-dotted curves). It only contributes significantly at very backward and forward angles. Around $\theta_\pi = 90°$ the main contribution comes from the non-spin-flip transition associated with the elementary amplitude f_2 which is dominated by the Δ resonance.

The role of the rescattering mechanism can be seen by comparing the simple PWIA (dashed curves) with our full calculations (solid curves). Its contribution is biggest in the Δ-resonance region and at backward angles. Among the different rescattering mechanisms elastic scattering (without charge exchange) dominates in this energy region. This is in contrast to the threshold region where, as we have seen above, charge exchange rescattering gives the main contribution. Above the Δ-resonance region, the rescattering contribution becomes smaller with increasing photon energy.

The role of the $^3D_1$ configuration in the deuteron wave function is also illustrated in Fig. 4 by turning off the nuclear matrix elements with $L = 2$. The D-wave contribution becomes manifest at large angles, $\theta_\pi > 90°$, for energies $E_\gamma > 300$ MeV, which corresponds to momentum transfers of $Q^2 > 3.1$ fm^{-2}.

We conclude our analysis of the differential cross section by comparing with previous calculations. Our results presented here are very similar to the ones obtained by Bosted and Laget [2]. The main difference between our and their approach is the treatment of the pion rescattering contributions. In our formalism the coupling with the breakup channels was not included in contrast to Ref. [2]. Apparently, the corresponding contribution is small in the kinematical range considered here.

A comparison with the Garcilazo and Guerra [6] calculations shows that in the forward direction their results are generally about 50% larger, except at $E_\gamma = 340$ MeV. This could indicate a difference in the spin-flip part of the elementary amplitude which dominates in the forward direction. Below we show that this leads to a dramatic difference in the vector analyzing power. The work by Blaazer [7] includes only a comparison with the data at $E_\gamma = 300$ MeV. Their results are about 20% above the measured cross section. Within their Faddeev formalism they find only small pion rescattering effects. Compared to the calculations by Wilhelm and Arenhövel [5] our results are lower and agree better with the data, except for $\theta_\pi = 6°$. The main reason for this difference is due to pion rescattering in our approach which reduces the cross sections considerably in the region of the Δ resonance (see Fig. 4).

B. Polarization observables

Photon asymmetry. Figure 5 shows the angular distribution for the photon asymmetry calculated at $E_\gamma = 200$–400 MeV in PWIA (dashed curves) and DWIA (solid curves). The dotted curves are DWIA calculations without the D-state configuration in the deuteron wave function. Clearly, all calculations are very similar; thus, the influence of the deuteron D-state and pion rescattering is small. Moreover, our analysis showed that the contribution of the $l = 2$ multipoles in the elementary production amplitude is also negli-

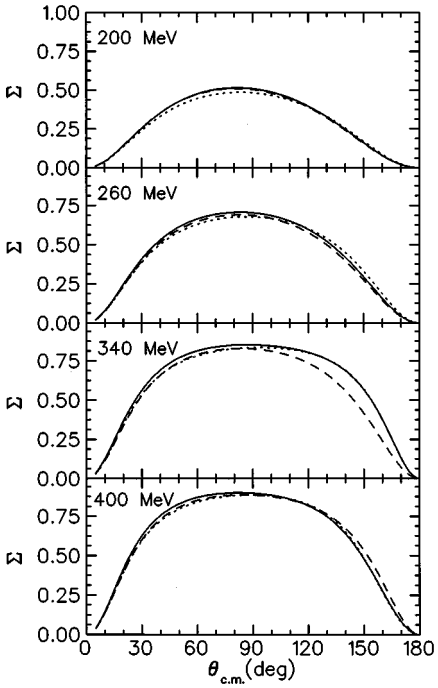

FIG. 5. Photon asymmetry Σ at E_γ=200–400 MeV. The solid and dashed curves are full and PWIA calculations, respectively. The dotted curves are obtained without deuteron D state.

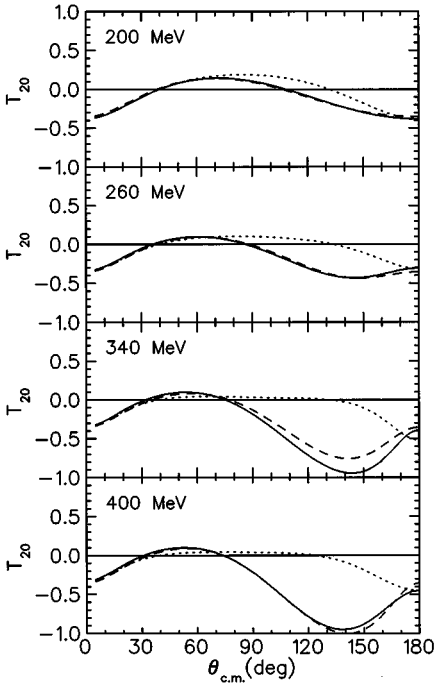

FIG. 6. Tensor analyzing power T_{20}. The notations of the curves are as in Fig. 5.

gible, e.g., we can set $f_4=0$. Thus, using Eq. (24) the photon asymmetry can be expressed in a rather simple form using only the elementary amplitudes f_1, f_2, and f_3:

$$\Sigma^{(S)}(\text{deuteron}) \approx \tfrac{3}{4}\sin^2\theta_\pi \frac{|f_2|^2 - \tfrac{2}{3}|f_3|^2}{|f_1|^2 + \tfrac{3}{4}\sin^2\theta_\pi(|f_2|^2 + \tfrac{2}{3}|f_3|^2)}. \quad (28)$$

This expression is close to the expression for the elementary photon asymmetry for the process on the nucleon:

$$\Sigma(\text{nucleon}) \approx \tfrac{1}{2}\sin^2\theta_\pi \frac{|f_2|^2 - |f_3|^2}{|f_1|^2 + \tfrac{1}{2}\sin^2\theta_\pi(|f_2|^2 + |f_3|^2)}. \quad (29)$$

Therefore, the angular distribution of the photon asymmetry for the production process on hydrogen and deuteron looks very similar.

Tensor analyzing powers. Figure 6 presents our results for the T_{20} observable obtained in the same way as the photon asymmetry. However, in contrast to the photon asymmetry, T_{20} is very sensitive to the deuteron D-state component (compare solid and dotted curves). The influence of pion rescattering still remains small.

In the region of $90° < \theta_\pi < 150°$, where the contribution of the D state is more important the value for T_{20} can be estimated from Eq. (24) as

$$T_{20}(\sim 130°) \approx \frac{|\mathcal{A}_M|^2 - |\mathcal{E}_M|^2}{|\mathcal{A}_M|^2 + \frac{1}{2}|\mathcal{E}_M|^2} \approx -(1+3\cos 2\Theta)\frac{x}{1+3x^2\sin^2 2\Theta}, \quad (30)$$

where angle Θ is defined in Eq. (25c) and $x = R_{02}^{(2)}(Q)/R_{00}^{(0)}(Q)$. This ratio describes the role of the deuteron D state as a function of the momentum transfer Q. It is clear that with increasing Q the ratio x also increases and $|T_{20}|$ reaches its maximum value.

The contribution of the deuteron S-state dominates at forward and backward angles. In this region $\mathcal{B}_M = \mathcal{D}_M = -\mathcal{B}_E = -\mathcal{D}_E$ and other amplitudes are zero. Therefore, independent of the photon energy we have

$$T_{20}(0°) \approx T_{20}(180°) \approx -\frac{\sqrt{2}}{4}. \quad (31)$$

As can be seen in Fig. 6, this relation is generally fulfilled and only small deviations appear due to pion rescattering and Fermi motion.

Thus we find that the maximum value of the tensor analyzing power T_{20} is only sensitive to the D-state component of the deuteron wave function and not to the details of the elementary amplitudes or to pion rescattering.

The behavior of the other tensor polarization observables T_{21} and T_{22} is similar (see Fig. 7 and Fig. 8). They both have a maximum negative value around $\theta_\pi = 90^0$. As in the case of T_{20} this value is determined by the deuteron D state. Using Eq. (24), this dependence can be expressed approximately as

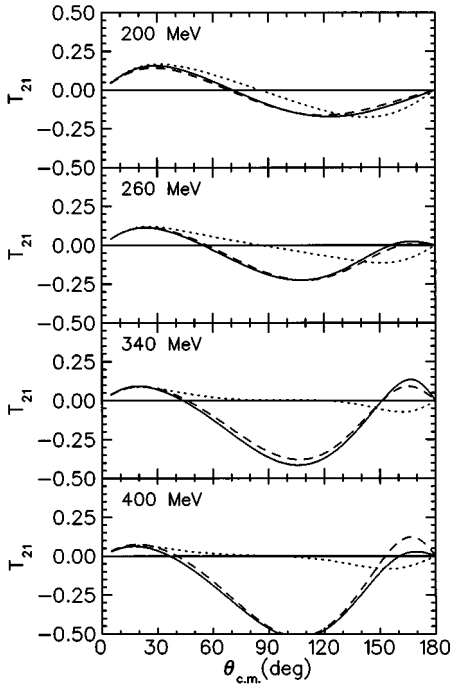

FIG. 7. Tensor analyzing power T_{21}. The notations of the curves are as in Fig. 5.

$$T_{21}(\sim 90°) \approx -\sqrt{6}\sin 2\Theta \frac{x}{1+3x^2\sin^2 2\Theta}, \tag{32a}$$

$$T_{22}(\sim 90°) \approx -\sqrt{3/2}(1-\cos 2\Theta)\frac{x}{1+3x^2\sin^2 2\Theta}. \tag{32b}$$

From this equation it follows that at the maximum $T_{21} \approx 2T_{22}$. In the forward and backward direction these observables vanish. At low energies the S-state component becomes visible and the D-state contribution is negligible. In this region, T_{21} can be estimated by the following expression:

$$T_{21}^{(S)}(E_\gamma \sim 200\ \text{MeV}) \approx -\frac{\sqrt{3}}{4}\sin\theta_\pi \frac{\mathrm{Re}[f_1^* f_3]}{|f_1|^2 + \frac{3}{4}\sin^2\theta_\pi(|f_2|^2 + \frac{2}{3}|f_3|^2)}. \tag{33}$$

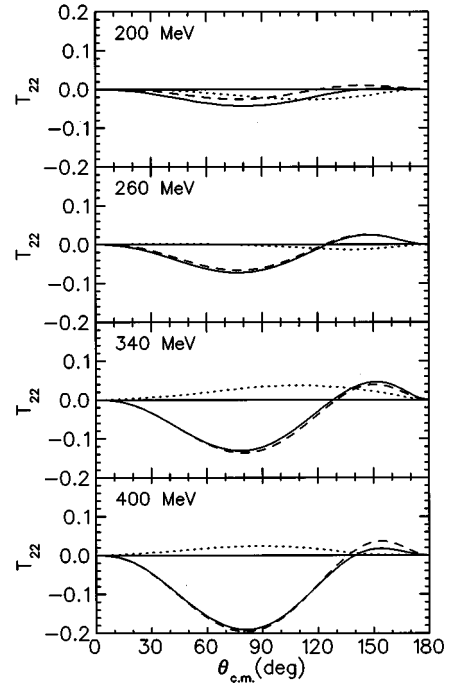

FIG. 8. Tensor analyzing power T_{22}. The notations of the curves are as in Fig. 5.

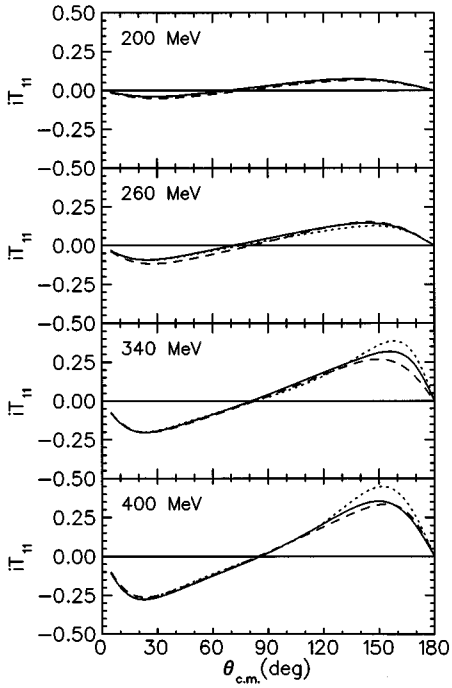

FIG. 9. Vector analyzing power T_{11}. The notations of the curves are as in Fig. 5.

Vector analyzing power. In our study of polarization observables in elastic pion-deuteron scattering (see paper I) we found that the vector analyzing power iT_{11} is very sensitive to the details of the theory. Especially pion rescattering was very important, around the Δ-resonance region it changed the sign of iT_{11}.

Our calculations, shown in Fig. 9, indicate that the influence of pion rescattering is not important for iT_{11} in the case of π° photoproduction (compare solid and dashed curves). The contribution of the deuteron D-state is also small. Therefore, in this reaction the vector analyzing power is neither sensitive to details of the rescattering mechanism nor to nuclear structure. Therefore, it can be expressed entirely through the elementary amplitudes $f_1, \ldots, f_4$. If we again neglect the small contribution from the f_4 amplitude iT_{11} has a simple form,

$$iT_{11}^{(S)}(\text{deuteron}) \approx -\frac{\sqrt{3}}{2}\sin\theta_\pi \times \frac{\mathrm{Im}[f_1^*(f_2 - \frac{1}{2}f_3)]}{|f_1|^2 + \frac{3}{4}\sin^2\theta_\pi(|f_2|^2 + \frac{2}{3}|f_3|^2)}. \tag{34}$$

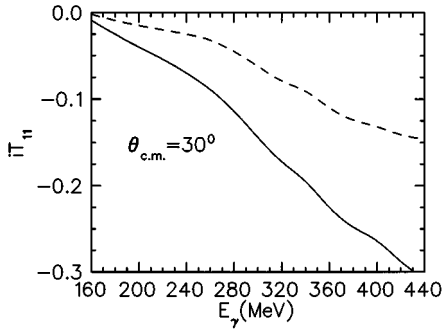

FIG. 10. Sensitivity of iT_{11} to the E_{1+}^{Δ} multipole. The solid and dashed curves are the results obtained with and without this multipole, respectively.

Furthermore, due to the small nonresonant E_{0+} multipole, f_1 reduces to

$$f_1 \approx \cos\theta_\pi (3E_{1+} + M_{1+} - M_{1-}). \tag{35}$$

Therefore, iT_{11} has a $\sin\theta_\pi \cos\theta_\pi$ angular dependence and changes the sign around $\theta_\pi = 90°$. Note that this result is in strong disagreement with the predictions of Garcilazo and Guerra [6]. Their vector analyzing power is positive in the Δ-resonance region at all angles. This can occur only through differences in the elementary amplitude. At the same time their predictions for the photon asymmetry and tensor analyzing powers are very similar to ours.

Another interesting consequence which comes from Eqs. (34) and (35) is related to the contribution of the E_{1+} multipole. It is of a particular interest because of its resonant part due to the $E2$ transition in the $\gamma N\Delta$ vertex. The size of this quadrupole component is very sensitive to the tensor force in the quark-quark interaction. Thus, this transition could give us a measure for the deformation of the delta and, subsequently, of the nucleon in the framework of quark models.

Figure 10 illustrates the sensitivity of the vector analyzing power to the contribution of the $E2$ transition in $\gamma N\Delta$ vertex at $\theta_\pi = 30°$. As follows from Fig. 9, the influence of other theoretical uncertainties is minimal in this region. However, the presence of the E_{1+}^{Δ} multipole dramatically changes the value of iT_{11}.

Note that a similar situation also occurs in $\pi°$ photoproduction on the nucleon. Again, if we neglect the small contribution from the f_4 amplitude we obtain for the target asymmetry on the proton

$$T = \sqrt{2} iT_{11}(\text{nucleon}) \approx -\sin\theta_\pi \frac{\text{Im}[f_1^*(f_2 - f_3)]}{|f_1|^2 + \frac{1}{2}\sin^2\theta_\pi(|f_2|^2 + |f_3|^2)}. \tag{36}$$

V. η PHOTOPRODUCTION

We complete our analysis with an investigation of coherent η photoproduction on the deuteron. The formalism for this process can be developed in a straightforward way by the same coupled channels method which has been applied to pion photoproduction. In momentum space the nuclear photoproduction amplitude can be written as

$$F_{\eta\gamma}^{(\lambda)}(\vec{q},\vec{k}) = V_{\eta\gamma}^{(\lambda)}(\vec{q},\vec{k}) - \frac{a}{(2\pi)^2} \times \sum_{i=\pi,\eta} \int \frac{d^3q'}{\mathcal{M}_i(q')} \frac{F_{\eta i}(\vec{q},\vec{q}\,')V_{i\gamma}^{(\lambda)}(\vec{q}\,',\vec{k})}{\mathcal{E}_\eta(q) - \mathcal{E}_i(q') + i\epsilon}, \tag{37}$$

where $\vec{k}$ is the photon, and $\vec{q}$ is the η or pion momentum. The total energy in the η-nucleus and π-nucleus channels is denoted by $\mathcal{E}_i(q) = E_i(q) + E_A(q)$, the reduced mass is given by $\mathcal{M}_i(q) = E_i(q)E_A(q)/\mathcal{E}_i(q)$, and $a = (A-1)/A$.

$V_{\eta\gamma}$ is expressed in terms of the free η-nucleon photoproduction t-matrix

$$V_{\eta\gamma}^{(\lambda)}(\vec{q},\vec{k}) = -\frac{\sqrt{\mathcal{M}_\eta(q)\mathcal{M}_\gamma(k)}}{2\pi} \times \left\langle \eta(\vec{q}), f \left| \sum_{j=1}^{A} t_{\eta\gamma}(j) \right| i, \gamma(\vec{k}\lambda) \right\rangle. \tag{38}$$

As an elementary $t_{\eta\gamma}$ amplitude we will use the extended dynamical model of Bennhold and Tanabe [34,35] where the resonance sector is constrained by solving the coupled channels problem for the $\pi N \to \pi N$, $\pi N \to \eta N$, $\pi N \to \pi\pi N$, and $\gamma N \to \pi N$ reactions, using available data as input. The background is formed by the contributions from s- and u-channel Born terms and by ρ- and ω- exchange in the t-channel. Following the analysis of Ref. [35] we use pseudoscalar Born terms with an ηNN coupling constant of $g_\eta^2/4\pi = 0.4$.

At present, little is known about the nature of the η-nucleus interaction which enters in the amplitude $F_{\eta i}(\vec{q},\vec{q}\,')$. For the elementary $\pi N \to \eta N$ process the experimental data is much less complete and accurate in contrast to πN-scattering data. There are only few theoretical studies of this reaction [34,36,37] based on the coupled channel isobar model for the $\pi N, \eta N$, and $\pi\pi N$ systems. More detailed information about the structure of the η-nucleus interaction can be found in our previous work [9]. We only note that, just as in pion photoproduction, the η scattering amplitude $F_{\eta i}$ is constructed as a solution of the Lippmann-Schwinger equation using the KMT version of multiple scattering theory. At present our calculations have been carried out in DWIA without coupling to the pion channel because our elementary pion photoproduction amplitude is not well appropriate for the photon energies $E_\gamma > 500$ MeV where higher nucleon resonances become important. From the other hand as it was estimated in Ref. [40] contributions coming from the pion channel are much smaller than eta rescattering terms.

In Fig. 11, we show the differential cross section for coherent η photoproduction on the deuteron at $E_\gamma = 675$ MeV (48 MeV above threshold). The reaction is completely dominated by the resonance contribution, the nonresonant Born terms and vector meson contributions are negligible. The η rescattering contribution in the final state is also small in this energy region.

Figure 12 presents the energy dependence of the differential cross section at $\theta = 90°$. Old experimental data [38] are in dramatic disagreement with numerous theoretical predictions [39–41]. This is related to the small isoscalar (γ, η)

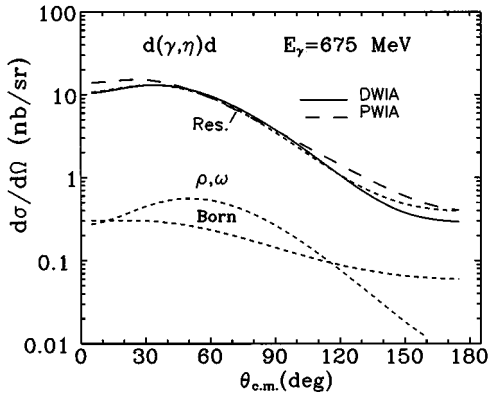

FIG. 11. Differential cross section for coherent η photoproduction on the deuteron at 675 MeV photon lab energy. The dotted curves show the individual contributions for the resonance excitation and the nonresonant background from vector mesons and Born terms in PWIA. The dashed and full lines give the full calculations in PWIA and DWIA, respectively.

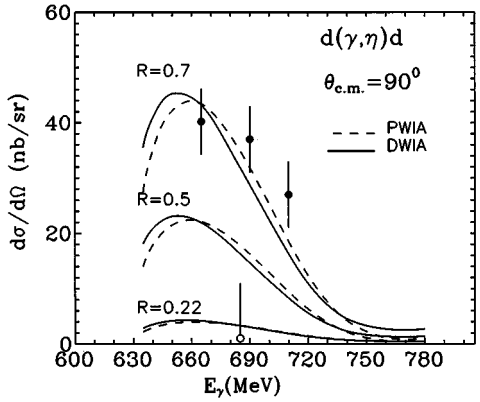

FIG. 12. Energy dependence of the differential cross section at fixed angles $\theta_\eta = 90°$ for the $d(\gamma,\eta)d$ reaction calculated with different ratios $R = E_{0+}^{(0)}/E_{0+}^{(p)} = 0.22$, 0.5, and 0.7, where the first value is the prediction of the Bennhold Tanabe model [34]. The dashed and solid curves are the PWIA and DWIA calculations, respectively. Experimental data are from Refs. [42] (o) and [38] (●).

amplitude $E_{0+}^{(0)}$ with $R = E_{0+}^{(0)}/E_{0+}^{(p)} = 0.22$. As can be seen in Fig. 12, only an unrealistically large isoscalar amplitude of $E_{0+}^{(0)}/E_{0+}^{(p)} = 0.7$ can explain the data. This puzzle was a subject of investigations by many authors over the past twenty years. Recently, a new experiment at Mainz by Krusche *et al.* [42] has obtained an upper limit for coherent η photoproduction which is in agreement with our calculations using a realistic ratio of $R \approx 0.2$. This is also confirmed by a preliminary analysis of an experiment at Bonn [43].

VI. CONCLUSION

In this paper we have presented a calculation for coherent pion and eta photoproduction from the deuteron using an approach that is consistent with the description of pion elastic scattering (paper I) [17]. The deuteron wave function used in our computation is obtained from the Paris potential. The final state interaction of the emitted mesons is treated in multiple scattering as described in paper I. All calculations are performed in momentum space treating dependence of the elementary amplitude from mesons and nucleon momenta exactly.

Our calculations agree well with existing data of differential cross sections and can also reproduce previous calculations found in the literature. In the case of π^0 photoproduction in the threshold region we have found significant sensitivity of the differential cross section to the $E_{0+}^{(+)}$ isospin amplitude of the nucleon that should allow a determination of the $E_{0+}(\pi^0 n)$ amplitude [44]. For coherent η photoproduction new experimental data from Mainz is in agreement with our results obtained using a realistic ratio of $E_{0+}^{(0)}/E_{0+}^{(p)} = 0.22$.

We have applied our approach to polarization observables that can be measured with the new electron scattering facilities where polarized targets and beams are becoming available. A number of simple relationships between polarization observables and the basic production amplitude was derived for the kinematical regions where nuclear structure and pion rescattering are not important. We found a strong sensitivity to the deuteron D-state component in the tensor analyzing powers. The vector analyzing power (iT_{11}) or target polarization shows an enhanced sensitivity to the resonant E_{1+}^{Δ} multipole. This very important quantity may give insight into the medium modification of baryons in the presence of other nucleons. A study of this amplitude is possible by looking at different nuclei. In a previous paper on ^{3}He it was found that this multipole can be rather easily observed with a polarized photon beam.

Up to now there are only few good data available for this rather elementary reaction and polarization observables are missing in the low energy and Δ region. With the new accelerators at Mainz, Bonn, Saskatoon and, very soon, CEBAF and the development of very powerful spectrometers and detectors we hope that soon precise data will become available, thus improving our knowledge of the production and interaction of mesons with very light nuclei.

ACKNOWLEDGMENTS

We would like to thank Henk Blok, Bernd Krusche, and Michael Fuchs for a fruitful discussion on threshold photoproduction. This work was supported by the Deutsche Forschungsgemeinschaft (SFB 201), the U.S. DOE Grant No. DE-FG02-95-ER40907, and the Heisenberg-Landau program.

APPENDIX

In this appendix we give PWIA expressions for the *Robson amplitudes* $\mathcal{A}, \ldots, \mathcal{E}$ with the deuteron S and D states taken into account. They are expressed with nuclear matrix elements $M_{SLJ}(Q)$ defined in Ref. [17]

$$M_{000}(Q) = 2\sqrt{3/4\pi}[R_{00}^{(0)}(Q) + R_{22}^{(0)}(Q)], \qquad \text{(A1)}$$

$$M_{022}(Q)=4\sqrt{3/4\pi}\left[R_{02}^{(2)}(Q)-\frac{\sqrt{2}}{4}R_{22}^{(2)}(Q)\right], \quad \text{(A2)}$$

$$M_{101}(Q)=2\sqrt{6/4\pi}\left[R_{00}^{(0)}(Q)-\frac{1}{2}R_{22}^{(0)}(Q)\right], \quad \text{(A3)}$$

$$M_{121}(Q)=-2\sqrt{6/4\pi}\left[R_{02}^{(2)}(Q)+\frac{1}{\sqrt{2}}R_{22}^{(2)}(Q)\right]. \quad \text{(A4)}$$

For the magnetic part of the $\mathcal{A},\ldots,\mathcal{E}$ amplitudes in the PWIA approach we obtain

$$\mathcal{A}_M=\sqrt{4\pi/6}f_2\sin\theta_\pi^*\left[M_{000}(Q)-\frac{1}{4\sqrt{2}}(1+3\cos2\Theta)M_{022}(Q)\right]W_A, \quad \text{(A5)}$$

$$\mathcal{B}_M=\tfrac{1}{2}\sqrt{4\pi/6}[f_1M_S(Q)+\tfrac{3}{2}f_2\sin\theta_\pi^*\sin2\Theta M_{022}(Q)]W_A, \quad \text{(A6)}$$

$$\mathcal{C}_M=-\tfrac{3}{8}\sqrt{4\pi/3}f_2\sin\theta_\pi^*(1-\cos2\Theta)M_{022}(Q)W_A, \quad \text{(A7)}$$

$$\mathcal{D}_M=-\tfrac{1}{2}\sqrt{4\pi/6}[f_1M_S(Q)-\tfrac{3}{2}f_2\sin\theta_\pi^*\sin2\Theta M_{022}(Q)]W_A, \quad \text{(A8)}$$

$$\mathcal{E}_M=\sqrt{4\pi/6}f_2\sin\theta_\pi^*\left[M_{000}(Q)+\frac{1}{2\sqrt{2}}(1+3\cos2\Theta)M_{022}(Q)\right]W_A. \quad \text{(A9)}$$

For the electric part we obtain

$$\mathcal{A}_E=-\tfrac{1}{2}\sqrt{4\pi/3}\sin\theta_\pi^*\left[(f_3+f_4\cos\theta_\pi^*)M_S(Q)-\frac{3}{\sqrt{2}}f_Q\cos\Theta M_{121}(Q)\right]W_A, \quad \text{(A10)}$$

$$\mathcal{B}_E=\mathcal{D}_E=-\frac{1}{2}\sqrt{4\pi/6}\left[(f_1+f_4\sin^2\theta_\pi^*)M_S(Q)+\frac{3}{\sqrt{2}}f_Q\sin\theta_\pi^*\sin\Theta M_{121}(Q)\right]W_A. \quad \text{(A11)}$$

In the PWIA approach the electric amplitude $\mathcal{C}_E=0$ which contributes only in the presence of pion rescattering. In Eqs. (A5–A11) we used the notation

$$M_S(Q)=M_{101}(Q)-\frac{1}{\sqrt{2}}M_{121}(Q). \quad \text{(A12)}$$

[1] J. H. Koch and R. M. Woloshyn, Phys. Rev. C **16**, 1968 (1977).
[2] P. Bosted and J. M. Laget, Nucl. Phys. **A296**, 413 (1978).
[3] H. Garcilazo and T. Mizutani, *πNN Systems* (World Scientific, Singapore, 1990).
[4] P. Wilhelm and H. Arenhövel, Few-Body Syst. Suppl. **7**, 235 (1994).
[5] P. Wilhelm and H. Arenhövel, Nucl. Phys. **A593**, 435 (1995).
[6] H. Garcilazo and E. M. Guerra, Phys. Rev. C **52**, 49 (1995).
[7] F. Blaazer, Ph.D. thesis, Free University of Amsterdam, 1995.
[8] S. S. Kamalov, L. Tiator, and C. Bennhold Phys. Rev. C **55**, 88 (1997), the preceding paper.
[9] S. S. Kamalov, L. Tiator, and C. Bennhold, Phys. Rev. C **47**, 941 (1993).
[10] S. S. Kamalov, L. Tiator, and C. Bennhold, Nucl. Phys. **A547**, 559 (1992).
[11] S. S. Kamalov, L. Tiator, and C. Bennhold, Few Body Syst. **10**, 143 (1991).
[12] A. K. Kerman, H. McManus, and R. M. Thaler, Ann. Phys. (N.Y.) **8**, 551 (1959).
[13] M. L. Goldberger and K. M. Watson, *Collision Theory* (Wiley, New York, 1964).
[14] G. F. Chew, M. L. Goldberger, F. E. Low, and Y. Nambu, Phys. Rev. **106**, 1345 (1957).
[15] I. Blomqvist and J. M. Laget, Nucl. Phys. **A280**, 405 (1977).
[16] J. M. Laget, Nucl. Phys. **A481**, 765 (1988).
[17] S. S. Kamalov, L. Tiator, and C. Bennhold, Phys. Rev. Lett. **75**, 1288 (1995).
[18] B. K. Jennings, Phys. Lett. B **205**, 187 (1988).
[19] A. S. Raskin, E. L. Tamusiak, and J. L. Friar, Few Body Syst. **17**, 71 (1994).
[20] L. Tiator and L. E. Wright, Phys. Rev. C **30**, 989 (1984).
[21] R. A. Eramzhyan, M. Gmitro, and S. S. Kamalov, Phys. Rev. C **41**, 2865 (1991).
[22] *Proceeding of the Third International Symposium on Polarization Phenomena in Nuclear Reactions*, edited by H. H. Barschall and W. Haelberli (University of Wisconsin Press, Madison, 1971).
[23] B. A. Robson, *The Theory of Polarization Phenomena* (Clarendon Press, Oxford, 1974).
[24] J. M. Laget, Phys. Rep. **69**, 1 (1981).
[25] P. Argan *et al.*, Phys. Lett. B **206**, 4 (1988); J. M. Bergstrom, in *Proceedings of the VII Miniconference on Electromagnetic Production of Mesons on Nucleon and Nuclei*, Amsterdam, 1991, edited by H. P. Blok, J. H. Koch, and H. de Vries (NIKHEF, Amsterdam, 1992), pp. 22–44.
[26] E. Mazzucato *et al.*, Phys. Rev. Lett. **57**, 3144 (1986).
[27] R. Beck, F. Kalleicher, B. Schoch, J. Vogt, G. Koch, H. Ströher, V. Metag, J. C. McGeorge, J. D. Kelle, and S. J. Hall, Phys. Rev. Lett. **65**, 1841 (1990).
[28] D. Drechsel and L. Tiator, J. Phys. G **18**, 449 (1992).
[29] V. Bernard, N. Kaiser, and U.-G. Meissner, Report No. CRN 94-62.

[30] E. Hilger, H.-J. Roegler, L. M. Simons, and M. Tonutti, Nucl. Phys. **B93**, 7 (1975).
[31] E. Holtey, G. Knop, H. Stein, J. Stümpfig, and H. Wahlen, Z. Phys. **259**, 51 (1973).
[32] W. Beulerz, thesis, Bonn University, 1994.
[33] B. Bouquet, J. Buon, B. Grelaud, H. N'guyen'goc, P. Petroff, R. Riskalla, and R. Tchapoutian, Nucl. Phys. **B79**, 45 (1974).
[34] C. Bennhold and H. Tanabe, Nucl. Phys. **A530**, 625 (1991).
[35] L. Tiator, C. Bennhold, and S. S. Kamalov, Nucl. Phys. **A580**, 455 (1994).
[36] R. S. Bhalerao and L. C. Liu, Phys. Rev. Lett. **54**, 865 (1985).
[37] H. C. Chang, E. Oset, and L. C. Liu, Phys. Rev. C **44**, 738 (1991).
[38] R. L. Anderson and R. Prepost, Phys. Rev. Lett. **23**, 46 (1969).
[39] N. Hoshi, H. Hyuga, and K. Kubodera, Nucl. Phys. **A324**, 234 (1979).
[40] D. Halderson and A. S. Rosental, Nucl. Phys. **A501**, 856 (1989).
[41] D. Halderson and A. S. Rosental, Phys. Rev. C **42**, 2584 (1990).
[42] B. Krusche *et al.*, Phys. Lett. B **358**, 40 (1995).
[43] G. Anton, Proceedings of the Sixth International Symposium on Meson-Nucleon Physics and the Structure of the Nucleon, Blaubeuren, Germany, 1995 [πN-Newsletters **10**, 74 (1995)].
[44] H. P. Blok *et al.*, ''π^0 Electroproduction near Threshold on the Deuteron,'' NIKHEF-K experimental proposal NR: 94-07.